July 27, 2000

Nonthermal Flare Emission from MeV-energy Electrons at 17, 34 and 86 GHz

M. R. Kundu[1], S. M. White[1], K. Shibasaki[2], & T. Sakurai[3]

ABSTRACT

We present analyses of two solar flares observed with high spatial resolution at 86 GHz with the BIMA millimeter–wavelength telescope and at 17 and 34 GHz with the Nobeyama radioheliograph. The flares were observed on Nov. 24, 1998 and May 1, 1999. At millimeter wavelengths these are impulsive events and therefore they must be produced by MeV energy electrons. The present study using simultaneous observations of two flares at 86, 34, and 17 GHz provides an excellent opportunity to study high–energy electrons with high–spatial–resolution observations at three optically–thin frequencies. The morphology of millimeter emission can reveal both the properties of the MeV–energy electrons and the nature of the coronal magnetic field lines where they radiate. One of the two events we present is the first clear case of a $\lambda = 3$ mm source in which both footpoints of a loop are detected. In the second event the polarization image at 17 GHz also suggests a bipolar or loop–like morphology. Such morphological observations can be used to constrain the nature of the magnetic field in the solar corona.

Subject headings: Sun: flares, radio radiation, corona

1. INTRODUCTION

The importance of millimeter-wavelength observations is that in the impulsive phase they are only sensitive to the most energetic electrons accelerated by solar flares, and not

[1]Astronomy Department, University of Maryland, College Park, MD 20742

[2]Nobeyama Radio Observatory, NAO, Minamisaku, Nagano 384-13, Japan

[3]National Astronomical Observatory, Mitaka, 181-8588 Japan

the electrons in the energy range below 500 keV which can dominate microwave emission. This fact results from the combination of the characteristics of the mechanism which produces the impulsive radio emission from solar flares (gyroresonance emission, i.e., radiation due to the acceleration of electrons spiraling in a magnetic field), and the range of magnetic field strengths typical of the corona. Gyroresonance emission takes place at harmonics of the local gyrofrequency, broadened by thermal motion. Typical coronal gyrofrequencies have an upper limit of order 5 GHz, so that any gyroemission at our observing frequency (86 GHz, wavelength 3.5 mm) must be produced at gyroharmonics of at least 20, and usually higher. Indeed, quantitative calculations verify the conclusion that only MeV-energy electrons can produce significant gyrosynchrotron emission at 3 mm wavelength (White & Kundu 1992). These electrons radiate strongly at millimeter wavelengths and this makes millimeter observations a much more sensitive diagnostic of MeV electrons than are gamma-ray observations. Millimeter interferometers are sensitive enough to detect such high energy electrons even in small flares, and they are commonly produced in flares of all sizes. There is evidence that typical flare energy spectra show a "break downwards" slightly above the 20 - 100 keV energy range, with the spectrum becoming steeper at high energies. On the other hand, observations of the radio spectrum out to millimeter wavelengths suggest the opposite result: namely, that there is a flattening of the electron energy spectrum at high energies ($\gtrsim$ 1 MeV), required to explain the relatively large millimeter fluxes BIMA has detected. The combination of these two results suggests that there are several distinct electron populations produced in flares: the 20 - 100 keV population, which receives the bulk of the energy converted to electron kinetic energy; and a hard component which typically has a flatter spectrum. Indeed, it will be important to image flaring loops as a function of electron energy. We do not presently understand the relationship between these two components of the electron population. It is possible that the high-energy population is produced by the same physical mechanism as the lower-energy population, but operating in a different parameter regime, or they could be completely independent, or the lower-energy population may be required as a "seed" population, without which the mechanism for the production of the higher-energy population cannot get started. It is important to investigate further this problem with multiwavelength studies. In this paper we present two events which have been imaged both by the BIMA millimeter interferometer at 86 GHz and by the Nobeyama radioheliograph (NoRH) at 17 and 34 GHz. The two telescopes have similar resolution (here $10'' - 12''$). We also use Nobeyama patrol polarimeter data at several frequencies in the range 1 – 9.4 GHz. The importance of having images at such high frequencies is that the high–frequency radio spectrum can be reliably determined for different structures within the flare source. The two events discussed here have quite contrasting properties and are used to investigate the properties of energetic electrons in solar flares.

2. OBSERVATIONS

At the present time BIMA consists of 10 antennas (6-m dishes) located on E-W and N-S baselines. The relatively large number of the antennas results in a good instantaneous spatial coverage of the telescope, with a synthesized beam size which for our flares was about $7'' \times 6''$. The BIMA images at 86 GHz presented in this paper were made by first carrying out a preflare subtraction of the visibilities, and then mapping and self-calibrating the resulting data set. The nominal signal-to-noise achieved in these maps was of order 100, which roughly matches that achieved with other multi–element interferometers for snapshot imaging of flares.

The observations used in this paper are those of two flares obtained with the BIMA telescope, along with simultaneous microwave imaging data obtained with the Nobeyama Radio Heliograph (NoRH) at 17 and 34 GHz. The radio observations at 17 GHz were made with a spatial resolution of $10''$ and a temporal resolution of 1 s. The NoRH consists of 84 paraboloidal antennas, each antenna being 80 cm in diameter. They are located in a T-shaped array (east-west and north-south). The NoRH records both right-handed and left-handed circular polarization and has a field of view of $43'$ at 34 GHz covering the entire Sun. It has a dynamic range of better than 25 dB, and in the snapshot mode (1 s time resolution) it has a sensitivity of 4.4×10^{-3} sfu for a point source (Koshiishi et al. 1994; Enome et al. 1994; Shibasaki et al. 1994). The 17 GHz NoRH data were mapped in AIPS using techniques developed by T. Bastian and K. Shibasaki, described in Nindos et al. (1999). The 34 GHz NoRH data were mapped using standard NoRH routines.

For context information we also used data from telescopes on the SOHO satellite: 195 Å images from the Extreme ultraviolet Imaging Telescope (EIT) and longitudinal magnetograms from the Michelson Doppler Imager (MDI). Neither Yohkoh nor Compton Gamma Ray Observatory hard X–ray data are available near the time of the flare.

3. EVENT OF 1998 NOVEMBER 24

This was a northern winter event occurring at 23:42 UT: the Sun was at 8° elevation at BIMA at the time and was low on the eastern horizon at Nobeyama. The GOES soft X–ray class of this event was C2.9 and it occurred at heliographic coordinates S16E57. Figure 1 shows radio and soft X–ray time profiles for the event. The microwave data show very spiky time profiles and a very brief duration. The soft X–ray profile shows several stages: a preflare rise at 23:40:00, a steeper rise from 23:40:20 to 23:40:45, a more gradual rise from 23:40:45 (when the bright microwave peaks begin) to the GOES peak at 23:42:20, and then a steady decay. From the microwave fluxes it appears that this event had a low–frequency spectral peak (between 4 and 9 GHz); the flux at 17 GHz is small although the time profile matches that of the lower frequencies. At 86 GHz the BIMA data show a more gradual time profile and a peak flux stronger than at 17 GHz, but the time of the 86 GHz peak matches that of the 17 GHz peak. The 86 GHz time profile does not match the GOES time profile, so the 86 GHz emission from this event does not appear to be purely thermal free–free emission from the soft X–ray–emitting plasma as in some other events (Kundu et al. 1994). The event was too weak to be detected at 34 GHz by either the radioheliograph or the polarimeter.

Images of the flare are shown in Figure 2. This flare in NOAA 8393 was observed in Hα with the Solar Flare Telescope (Sakurai et al. 1995) of NAOJ/Mitaka. Magnetograms of this region were also obtained with the Solar Flare Telescope and by SOHO/MDI. The region is a bipolar group with two preceding spots of negative polarity and several following spots of positive polarity. The magnetogram shows a patch of parasitic positive polarity at the northern edge of the leading negative spot which is seen to be growing in a movie of MDI images. This site of emerging flux is the flare location. Hα flare recording started at 23:29 and lasted till 00:02 of November 25 in 30 s cadence. The initial brightening was seen at the north-east edge of the penumbra of the main preceding sunspot at 23:41. Then an ejection of material toward the north-east was observed. This surge phenomenon lasted for 8 minutes. The apparent lateral speed of the ejection is 190 km s^{-1}. At 23:49, when the surge was about to fade, its extent was 9×10^4 km. The surge activity originated presumably from the emergence of parasitic positive magnetic flux. The second peak of radio emission at 23:42:40 does not have a clear counterpart in the Hα observations. It may be related to the observed brightening of the leading front of the surge near this time.

17 GHz and 86 GHz images of the flare are shown in Figure 2, together with an EIT 195 Å image acquired at 23:48 UT, 7 minutes after the flare peak. The accuracy of the co–registration of the images at different wavelengths is not better than about $10''$. The EIT image shows a very compact loop straddling the neutral line at the northern edge of the leading spot where the parasitic polarity emerges, right at the Hα flare site. The weather at BIMA was poor for millimeter observing on this particular day, and with the source at such a low elevation we would not place too much significance on the bipolar structure found by self–calibrating the 86 GHz data were it not for the fact that the 17 GHz NoRH images with similar resolution also show a similar bipolar structure. Note that the absolute position of the 86 GHz source is not well determined due to the weather conditions and the position shown is based on matching the 17 and 86 GHz images. This is the first event in which a clear double structure is seen in 86 GHz images of a solar flare. There is no polarization information in the BIMA data (since a single linear polarization is recorded), while the 17 GHz images show negative polarity both from the the main flare source at 17 GHz as well as from the

leading sunspot to the south–west of the flare which can be seen in the magnetogram to be of strong negative magnetic polarity. At 23:41:00 the flare source dominates the 17 GHz circular polarization map, but due to the spiky nature of the time profile, by the time of the images in Figure 2 (23:41:10) the flare source has faded somewhat and the sunspot is again the strongest source in the circular polarization image. The spiky time profiles at frequencies $\lesssim$ 17 GHz suggest that the emission at 17 GHz and lower frequencies is nonthermal.

While both the 17 and 86 GHz images of the flare appear to show two footpoints separated by $20''$, comparison with the EIT image indicates that these cannot be the footpoints of the main flaring loop in soft X–rays which is only $10''$ long and lies north–south straddling the neutral line. Rather, the radio images are elongated parallel to the neutral line, and we speculate that the north–eastern component of the radio emission is associated with the surge activity seen in this direction in the Hα images. It is possible that the north–eastern radio source is a footpoint of a longer loop system which is not bright at 195 Å but which is an essential part of the magnetic reconfiguration taking place during the flare. Hanaoka (1997, 1999) has studied a class of events in which two interacting loop systems are involved, one being very compact while the other is a longer loop system with one footpoint located adjacent to the compact loop, and this flare may be a similar event. The importance of observing two footpoints at high frequencies is in what it reveals about the coronal magnetic fields on which the energetic electrons producing the millimeter emission travel. Except in the largest flares, millimeter sources will be optically thin and the optical depth will largely determine the fluxes observed. Gyrosynchrotron emissivity (the mechanism by which nonthermal electrons emit at millimeter wavelengths) is a very strong function of magnetic field strength, but electrons trapped in a loop will mirror back and forth between heights of equal magnetic field strength at the two ends of the loop and thus the maximum field strength they experience will be the same at both ends. In this case the main determinant of optical depth for trapped electrons will be the angle θ between the line of sight and the magnetic field, and this could be quite different at the two ends of the loop. Gyrosynchrotron calculations suggest that the emissivity depends on, e.g., $\sin^2\theta$ for an E^{-4} energy distribution (e.g., Dulk 1985). Thus when the millimeter emission is due to electrons trapped in a loop, we expect the two ends of the loop to be bright but not equally so; there should be enough dynamic range in BIMA observations to detect both footpoints. On the other hand, directly precipitating electrons can experience very different field strengths in the two feet, and since emissivity $\propto \mathrm{B}^3$ for an E^{-4} energy distribution, the difference in flux between the two footpoints can be very large, perhaps more than the dynamic range which a snapshot BIMA observation can achieve. The ways in which the loop geometry can be derived from the radio morphology have been discussed in some detail by Alissandrakis & Preka-Papadema (1984), Preka-Papadema et al. (1997), Bastian et al. (1998), and Nindos et al. (2000). The fact that in this event we see both footpoints at 86 GHz implies that the region of the loop in which the nonthermal electrons radiate was quite symmetric in terms of both magnetic field distribution and inclination to the line of sight.

4. EVENT OF 1999 MAY 1

This event was a GOES class C3 flare occurring at N22W40 at 23:00 UT on 1999 May 1. Figure 3 shows the radio and soft X–ray time profiles of the event. The GOES profile for this event is very interesting. The initial rise is at 22:54 UT; the rise accelerates at 22:57 UT and then again at 22:59 UT before peaking at 23:00:30. Thus a number of energy releases seem to contribute to the event in soft X-rays.

The microwave profiles are equally interesting. A burst confined to low frequencies (see Fig. 3, 9.4 and 3.75 GHz) is seen at 22:57 UT corresponding to one jump in the GOES profile, and a second high–frequency burst is seen at 22:59 UT corresponding to the second jump in the GOES profile.

This event was clearly detected at 34 GHz by NoRH with a time profile matching that at 17 GHz. Unfortunately BIMA missed the high–frequency peak due to a calibration scan. Prior to the calibration scan BIMA sees a small rise corresponding to the low–frequency microwave peak; however, the BIMA emission is not impulsive and looks more like a reflection of the GOES profile, i.e. is probably thermal free–free emission. When BIMA returns after the calibration scan, it first sees a decay similar to that seen in microwaves and soft X-rays, but then after 23:04 an increase in the 86 GHz emission is seen, which is matched at 17 and 34 GHz. There is no corresponding feature in the GOES profile, so we believe that the radio emission is not thermal emission from post-flare 10^7 K material: it could be very flat-spectrum nonthermal emission, or else flat-spectrum thermal emission from cooler material which does not contribute significantly to the GOES profile. The difference between the solid line and the symbols in the 34 GHz time profile is a rough indication of the size of the source, and this sugests that the source was larger during the later stages of the event than in the impulsive rise.

Images of the emission at 86, 34 and 17 GHz at 23:02:00 UT are shown in Fig. 4, together with an EIT 195 Å image at 23:12 UT and a longitudinal magnetogram. The 17 GHz images show only weak polarization during the flare, but during this period the 17 GHz source is clearly bipolar, with a structure indicating that the two components are separated by less than a beam width. This suggests that the radio source is again a bipolar loop, but of a size too small to be clearly resolved at the available resolution. The location of the radio source is right at the neutral line visible in the magnetogram, and the orientation of the "radio neutral line" is consistent with the orientation of the photospheric neutral line, but the co–registration of the images is not accurate enough to be confident of exactly where the radio source lies in relation to the photospheric features. The 34 GHz source is unresolved with a beam of order $8''$, and no polarization images are available at 34 GHz. The 17 and 34 GHz sources are coincident with the BIMA 86 GHz source for most of the time, with some post-flare brightening at 17 GHz in a source to the north-west. The 17 GHz images do show some emission corresponding to the low-frequency event at 22:57, but the spatial location is identical to that of the main flare source. The EIT image some 10 minutes after the flare shows no bright feature, which is consistent with the duration of the event in the GOES time profile shown in Figure 3.

5. DISCUSSION

In the present study we have used simultaneous observations of two flares at 86, 34, and 17 GHz to provide an independent study of the hypothesis that millimeter burst emitting electrons form a population different from the microwave and hard X-ray emitting electrons. Our study is based upon the production of images at all three frequencies at selected points of burst time profiles, and a comparative analysis of their positions at various times. We have used two powerful radio telescopes for our study. The Nobeyama Radio Heliograph is a dedicated instrument for solar studies. At the present time BIMA telescope uses 10 6-meter antennas, thus providing good u-v coverage. It is capable of producing snapshot images of solar flares with excellent spatial resolution and dynamic range of up to 100. Note, however, that BIMA telescope is not a solar dedicated telescope.

The two events we have studied occurred on Nov. 24, 1998, 23:41 UT, and on May 1, 1999, 23:04 UT. We have shown that 86, 17 GHz and 34 GHz sources on May 1 are unresolved with beams of approximately $7''$, $10''$ and $5''$ respectively. At 86 GHz, we missed the main peak coincident with 17 and 34 GHz, but there is enhanced emission a few minutes later at 86 GHz, which is seen at 17 GHz but much weaker than the main peak. At 34 GHz NoRH sees the main peak, but not the secondary peak, probably due to lower sensitivity of NoRH at this frequency. Because of the existence of the pronounced second peak, we consider that there may be a separate population of energetic electrons producing 86 GHz emission, as in the case of August 16, 1996 flare studied by Raulin et al. (1999). As for the Nov. 24, 1998 event there is no doubt that we are dealing with nonthermal emission up to about 17 GHz, as evidenced by polarization and impulsive nature of the bursts at 17 GHz and lower frequencies. At 86 GHz we observe only a gradual burst encompassing the two impulsive bursts at frequencies below 17 GHz and a slow decay. However, the 86 GHz time profile does not quite match the GOES time profile at 1.5 - 10 keV and 3.5 - 25 keV. Therefore we consider that 86 GHz emission from this event is not purely thermal free-free emission from the soft X-ray emitting plasma as in some other events (Kundu et al. 1994).

The most important results from this first study of solar flares using high spatial resolution observations at three high frequencies are that we see clear evidence for bipolar (loop–like) structures in the radio emission, including the first case of an event in which the 86 GHz emission clearly shows two footpoints. This morphology has implications for the nature of the loops in which the energetic electrons are trapped (Preka-Papadema et al. 1997; Nindos et al. 2000) which will be explored in more detail with a larger sample of events.

Acknowledgments

This work was carried out while M. R. Kundu was a Visiting Professor at the National Astronomical Observatory, Mitaka, and he gratefully acknowledges their hospitality. Solar radio research at the University of Maryland is supported by NSF grants ATM 96-12738 and INT 98–19917 and NASA grants NAG 5-7370, NAG 5-6257 and NAG 5-7901. We thank the EIT and MDI teams for making their data available for use in projects such as this.

REFERENCES

Alissandrakis, C. E. & Preka-Papadema, P. 1984, Astron. Astrophys., 139, 507

Bastian, T. S., Benz, A. O., & Gary, D. E. 1998, Ann. Rev. Astron. Astrophys., 36, 131

Dulk, G. A. 1985, Ann. Rev. Astron. Astrophys., 23, 169

Enome, S., Nakajima, H., Shibasaki, K., Nishio, M., Takano, T., Hanaoka, Y., Torii, C., Shiomi, Y., Sekiguchi, H., , Bushimata, T., Kawashima, S., Shinohara, N., Irimajiri, Y., Koshiishi, H., Choi, Y.-S., Sakai, J., Takahashi, M., Takakura, T., Sakao, T., & Kosugi, T. 1994, Publ. Astron. Soc. Japan, 46, L27

Hanaoka, Y. 1997, Solar Phys., 173, 319

—. 1999, Publ. Astron. Soc. Japan, 51, 483

Koshiishi, H., Enome, S., Nakajima, H., Shibasaki, K., Nishio, M., Takano, T., Hanaoka, Y., Torii, C., Sekiguchi, H., Kawashima, S., Bushimata, T., Shinohara, N., Irimajiri, Y., & Shiomi, Y. 1994, Publ. Astron. Soc. Japan, 46, L33

Kundu, M. R., White, S. M., Gopalswamy, N., & Lim, J. 1994, Astrophys. J. Supp., 90, 599

Nindos, A., Kundu, M. R., White, S. M., Gary, D. E., Shibasaki, K., & Dere, K. P. 1999, Astrophys. J., 527, 415

Nindos, A., White, S. M., Kundu, M. R., & Gary, D. E. 2000, Astrophys. J., 533, 1053

Preka-Papadema, P., Alissandrakis, C. E., Dennis, B. R., & Kundu, M. R. 1997, Solar Phys., 172, 233

Raulin, J., White, S. M., Kundu, M. R., Silva, A. R., & Shibasaki, K. 1999, Astrophys. J., 522, 547

Sakurai, T., Ichimoto, K., Noshino, Y., Shinoda, K., Noguchi, M., Li, E. H. T., He, F., Mao, W., Lu, H., Ai, G., Zhao, Z., Kawakami, S., & Chae, J. 1995, Publ. Astron. Soc. Japan, 47, 81

Shibasaki, K., Enome, S., Nakajima, H., Nishio, M., Takano, T., Hanaoka, Y., Torii, C., Sekiguchi, H., , Kawashima, S., Bushimata, T., Shinohara, N., Koshiishi, H., Shiomi, Y., Irimajiri, Y., Leka, K. D., & Canfield, R. C. 1994, Publ. Astron. Soc. Japan, 46, L17

White, S. M. & Kundu, M. R. 1992, Solar Phys., 141, 347

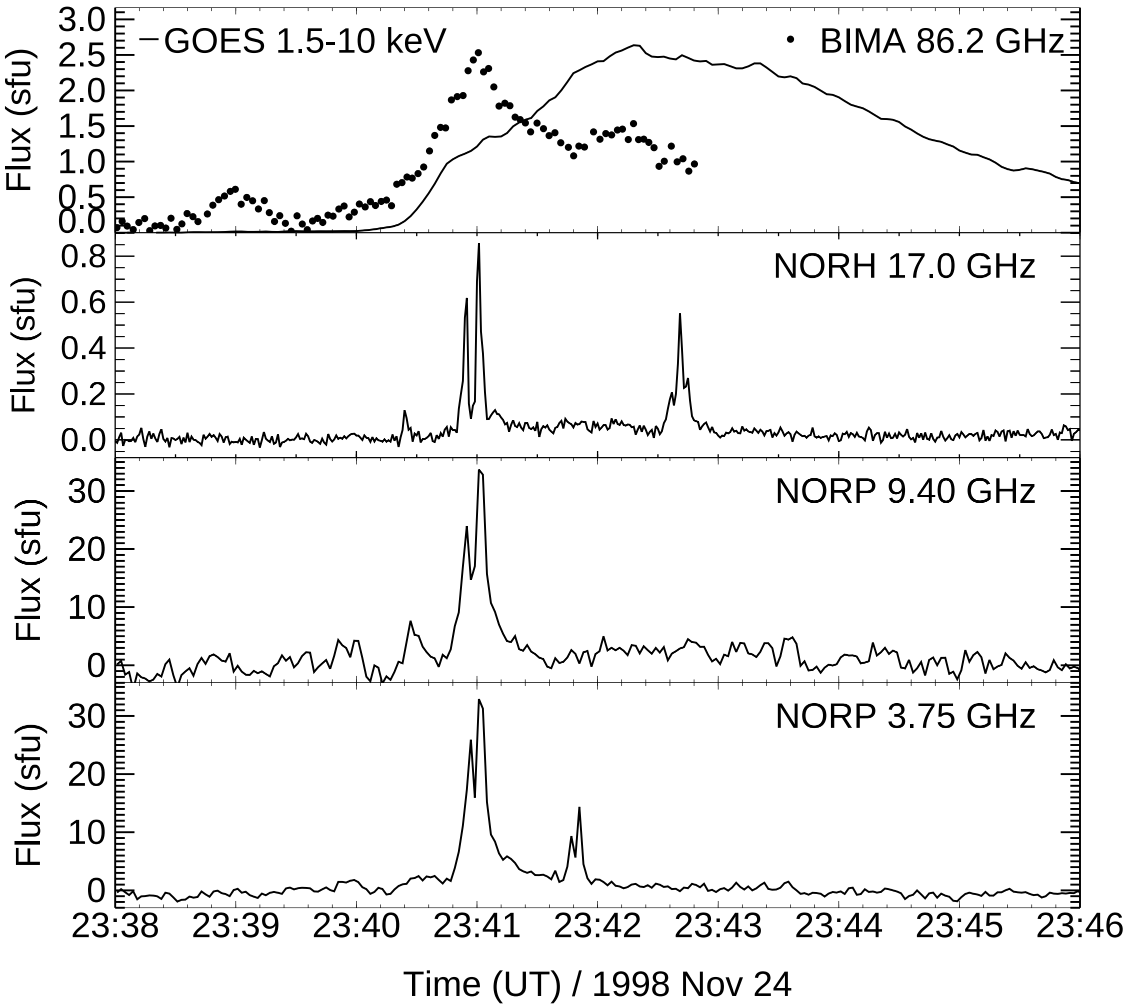

Fig. 1.— Radio and soft X–ray time profiles for the event of 1998 Nov. 24. The upper panel shows the BIMA flux at 86 GHz on the shortest baseline, which should represent the total flux of the event (dots), while the solid line is the GOES 1.5 – 10 keV channel time profile in a linear display. The second panel shows the NoRH 17 GHz time profile derived from the correlation coefficient, and the bottom two panels show the 9.4 and 3.75 GHz fluxes as measured by the Nobeyama polarimeters.

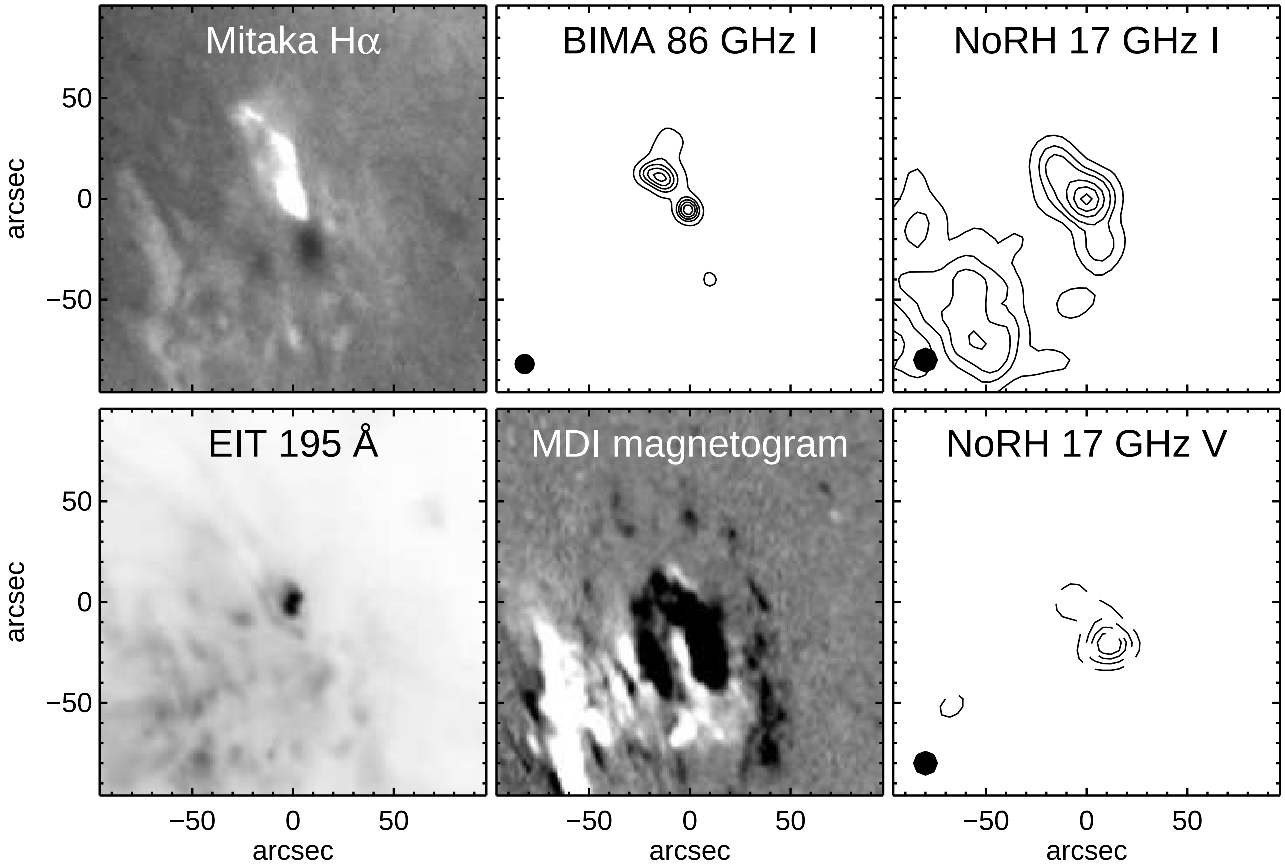

Fig. 2.— Images of the 1998 Nov. 24 flare at a number of wavelengths. The top left panel shows a line–center Hα image of the flare, and of the sunspot just south–west of the flare site, taken by by the Solar Flare Telescope at Mitaka, Japan, at 23:41:52 UT. The upper middle panel shows contours at 86 GHz from BIMA (one linear polarization, equivalent to total flux, left panel) at 23:41:20, and the two right–hand panels show NoRH 17 GHz images in total intensity (upper) and circularly–polarized flux (lower panel) at 23:41:10 UT. The bottom left panel shows an EIT 195 Å image obtained at 23:48 UT, and the lower middle panel shows an MDI magnetogram obtained at 22:24 UT with the display clipped at ± 150 G. The accuracy of the coregistration at different wavelengths is estimated to be accurate to better than 10″. The beam sizes in the radio images are 10″ at 86 GHz and 12″ at 17 GHz. Contours at 86 GHz are at levels of order 0.1 sfu per beam; at 17 GHz I, contours are at brightness temperatures of 20, 30, 40, 60, 80 and 100 $\times$ 10^3 K, and at 17 GHz V the contours are at brightness temperatures of 4, 8, 12, 16, 24, 32 and 40 $\times$ 10^3 K.

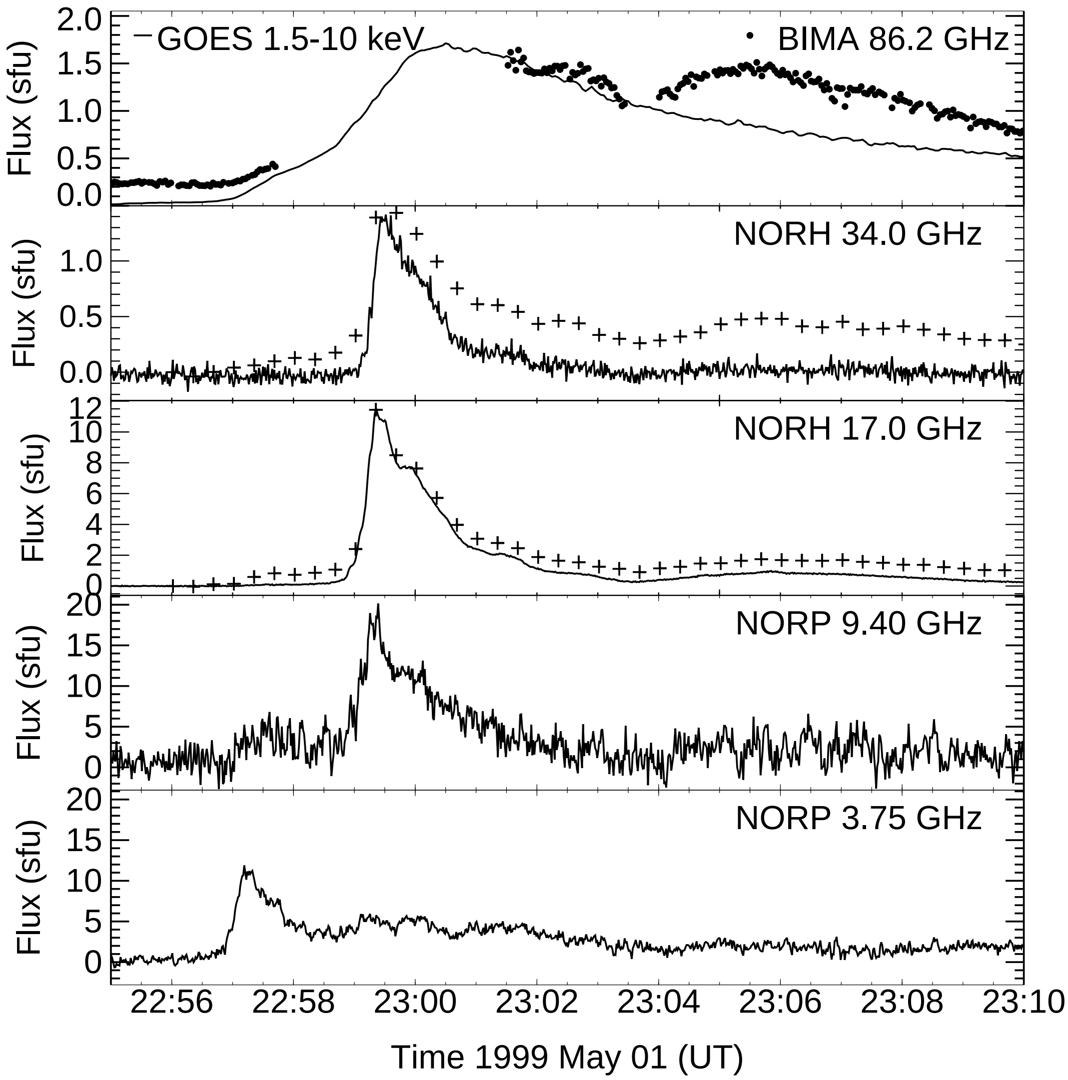

Fig. 3.— Radio and soft X–ray time profiles for the event of 1999 May 1 in the format of Fig. 1, with the addition of 34 GHz data from the Nobeyama radioheliograph. In the 17 and 34 GHz panels, the solid line is the 1 s correlation-plot data which samples only small spatial scales, while the plus symbols show total fluxes derived from images at specific times.

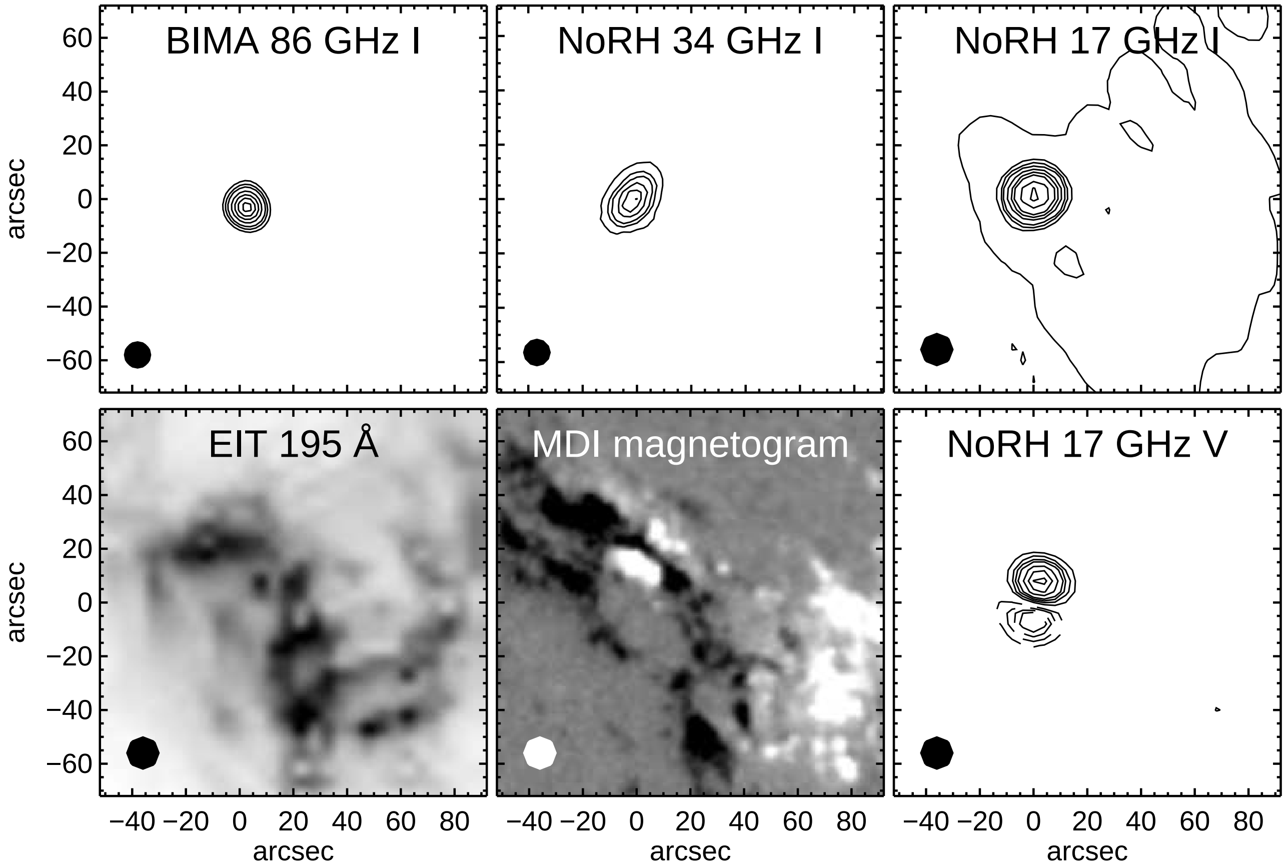

Fig. 4.— Images of the 1999 May 1 event at 23:02:00 UT. The format is similar to that of Fig. 2, with the exception that no Hα images are available and instead the middle upper panel shows the 34 GHz image from NoRH. The EIT 195 Å image was obtained at 23:12 UT, and the MDI magnetogram at 22:24 UT. The display of the magnetogram here is clipped at $\pm$ 300 G. 86 GHz contours are at approximately 0.1 sfu per beam, 34 GHz contours are plotted at 20, 30, 40, 60 & 80 $\times$ 10^3 K, 17 GHz I contours are plotted at .02, .2, .3, .4, .6, .8, 1, 1.5 and 2 $\times$ 10^6 K and 17 GHz V contours are plotted at 4, 8, 12, 16, 24, 32 and 40 $\times$ 10^3 K.